Middle Miocene back-arc volcanism in the Tappi-zaki area, Northeast Japan arc: plagioclase K-Ar age constraints

Naoki WATANABE*, Tetsumaru ITAYA**, Jun'ichi OHKI***
and Kenji SHUTO****

Abstract

K-Ar ages of whole rock and plagioclase separates were determined for Miocene volcanic rocks from the Tappi-zaki area, Tsugaru Peninsula in the Northeast Japan arc. Whole rock and plagioclase K-Ar ages for the basalt with subophitic groundmass are identical within analytical errors. On the other hand, whole rock K-Ar ages for the basalt, andesite and dacite with intersertal or hyalopilitic groundmass tend to be younger than those of plagioclase separates from the same samples. The discordance between whole rock and plagioclase K-Ar ages may be caused by radiogenic ^{40}Ar loss from whole rock due to alteration and hydration of glass in the groundmass. These suggest that the plagioclase K-Ar ages can be regarded as the formation ages of older volcanic rocks in the study area.

The obtained plagioclase K-Ar ages show that the extrusive rocks from the Tappi-zaki area, with a total thickness of about 1,500 m, were formed during 16.5-10 Ma (Middle to Late Miocene), and the dikes and sheets intruded these volcanic piles during the same period of 15-11 Ma. This implies that both the extrusive and intrusive rocks were produced by the same magmatic episode during the Middle to Late Miocene. The younger Minmaya rhyolites yielded a whole rock age of 7.9 Ma.

Key words: K-Ar dating, Minmaya rhyolites, Northeast Japan arc, Tappi-zaki, volcanic rocks

---

* Research Center for Natural Hazards and Disaster Recovery, Niigata University, Niigata 950-2181, Japan
** Research Institute of Natural Sciences, Okayama University of Science, Okayama 700-0005, Japan
*** Natural History Museum and Institute, Chiba, 260-8682, Japan
**** Department of Geology, Faculty of Science, Niigata University, Niigata 950-2181, Japan
(Manuscript received 24 December, 2008; accepted 3 March, 2009)

Introduction

Miocene volcanic rocks are distributed widely along the NE Japan arc. Recent geological, geochronological and petrochemical studies have revealed that the volcanism took place in a relatively short period from 13 to 16 Ma and its volcanic front was 30-50 km east of the Quaternary volcanic front (e.g., Uto et al., 1989; Shuto et al., 1993; Ohki et al., 1993a, b; Watanabe et al., 1993). The back-arc volcanism was also voluminous in the Middle Miocene but its temporal characterization is still vague because heavy alteration of the volcanic products has made it difficult to analyze ages precisely. This requires more sophisticated radiometric age determination of volcanic rocks to construct a more precise history of Miocene volcanism in the NE Japan arc.

The Miocene Tappi volcanic rocks distributed in the Tappi-zaki area of the northern Tsugaru Peninsula (Fig. 1) is clearly in the back-arc side if the Tomari volcanic rocks have formed on a volcanic front in the Middle Miocene volcanism (Watanabe et al., 1993). Stratigraphical studies of the Tappi volcanic sequence were carried out prior to the construction of the Seikan Tunnel under the Tsugaru Straits between the Tsugaru Peninsula in Honshu and the Oshima Peninsula in Hokkaido (Ota et al., 1957; Japan Railway Construction Corporation, Seikan Branch, 1989). As radiometric ages for the Tappi volcanic rocks, however, have not been reported yet, the eruptive history of Miocene volcanism in the Tappi-zaki area remains ambiguous.

This paper describes petrographical characteristics of the Tappi volcanic rocks, which collected systematically from the Tappi volcanic sequence and presents K-Ar ages of the groundmass rich fraction and the plagioclase phenocryst separates from these rocks. The paper further evaluates the age discrepancy between the two types of rock fraction, and then describes the back-arc volcanism during the Middle Miocene in the Tappi-zaki area on the basis of the plagioclase K-Ar ages and petrochemical data.

Outline of geology and petrology

The Tappi volcanic sequence distributed in the area of 10 km (N-S) $\times$9 km (E-W) of the northern Tsugaru Peninsula is composed of hyaloclastites associated with feeder dykes, massive lavas and their reworked deposits which suggest submarine eruption. The sequence, which is more than 1,500 m in maximum thickness, is lithologically divided into the four units; Horonai, Narugami, Tatsuhama and Sanyoushi (Fig. 2). The Horonai and Narugami units are in interfinger with each other and contemporaneous, and overlie conformably the Lower Miocene Fuyube Formation which is composed mainly of tuffaceous sandstones, siltstones and epiclastic volcanic rocks. The Tatsuhama and Sanyoushi units on the Narugami unit are likely contemporaneous because the lower parts of both units are in interfinger with the Narugami Unit. The Sanyoushi Unit is overlain conformably by the Middle to Upper Miocene Kodomari

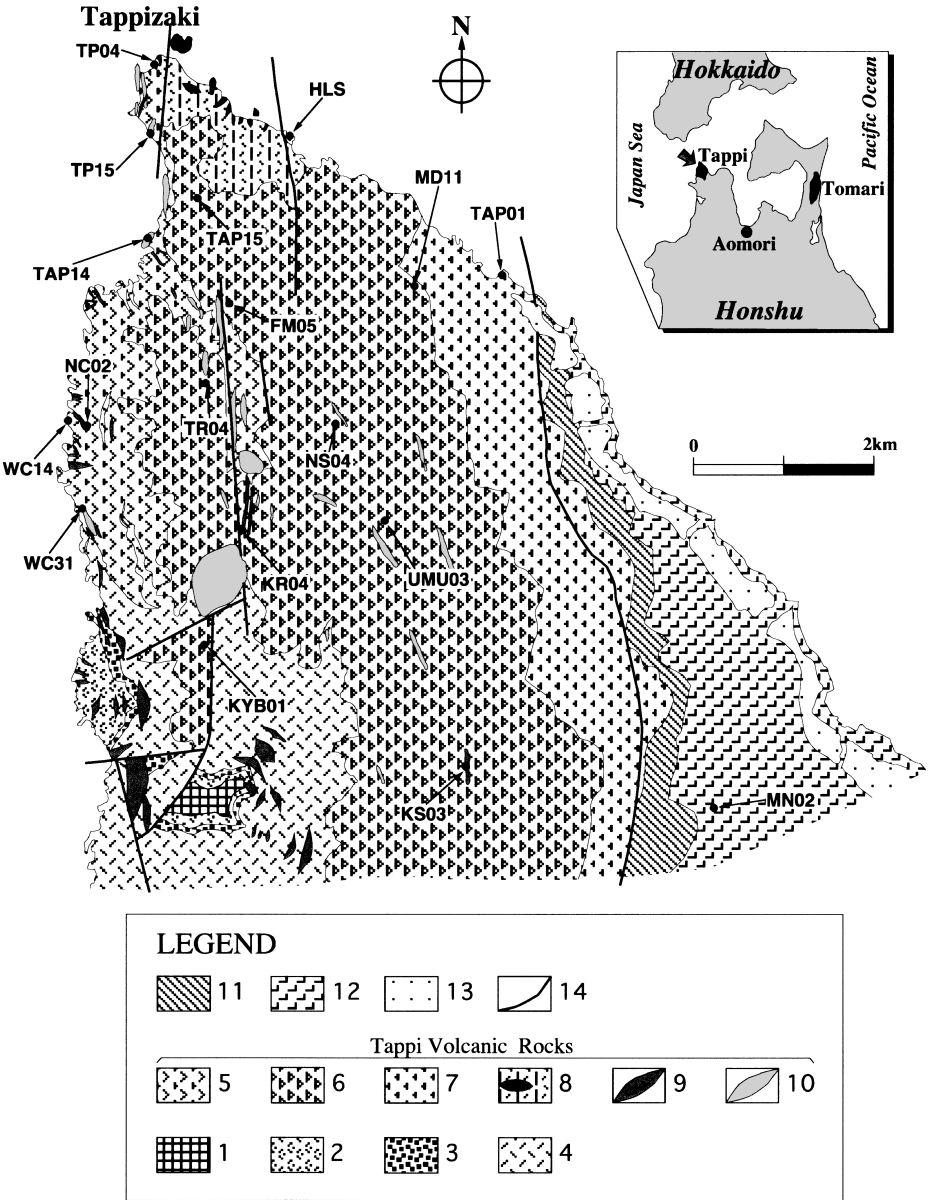

Fig. 1. Geological map of the Tappi-zaki area and sample localities for K-Ar dating. 1: Pre-Tertiary basement, 2: Gongenzaki Formation (Early Miocene), 3: Isomatsu Formation (Early Miocene), 4: Fuyube Formation (Early to Middle Miocene); 5-10: Tappi volcanic rocks (5: Horonai Unit, 6: Narugami Unit, 7: Sanyoushi Unit, 8: Tatsuhama Unit, 9: Dike and sheet of basalts and andesites, 10: Dike and sheet of dacites and rhyolites), 11: Kodomari Formation (Middle to Late Miocene), 12: Minmaya rhyolites, 13: Terrace deposits, 14: Fault.

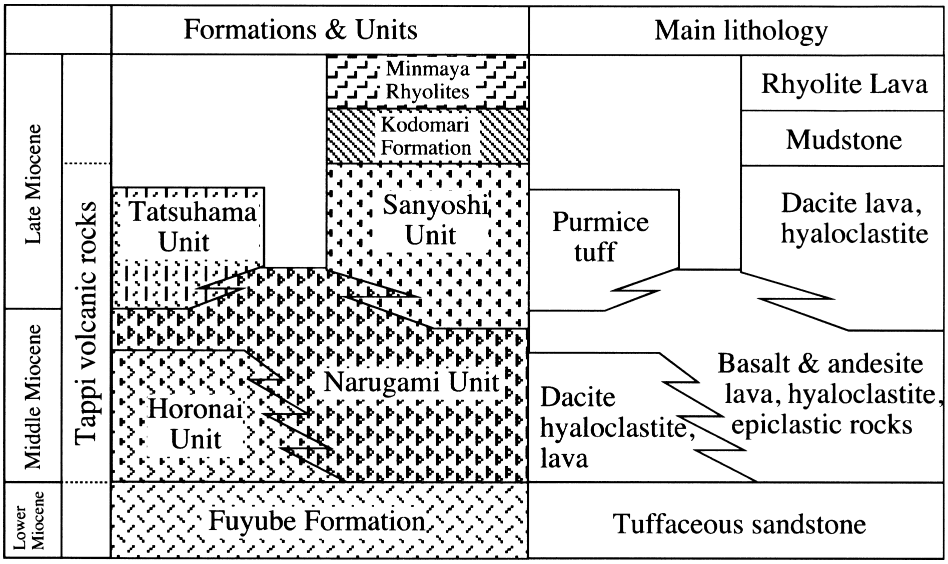

Fig. 2. Stratigraphic sequence of the Tappi-zaki area.

Formation which consists mainly of mudstone with intercalations of thin layers of tuffaceous sandstone. There are locally fault contact relations between the Sanyoushi Unit and the Kodomari Formation by the later deformation events. As the Narugami Unit is a predominant distribution in the sequence (Fig. 1), the main volcanism in the Tappi-zaki area should be occurred during the stage of the Narugami Unit.

The Horonai Unit is composed mostly of clinopyroxene-orthopyroxene dacites and the Narugami Unit is composed of olivine basalt, olivine-clinopyroxene basalt and orthopyroxene-clinopyroxene andesite. The Tatsuhama Unit consists of mainly dacitic tuff colored in light green, pumice tuff and tuff breccia. The Sanyoushi Unit comprises main clinopyroxene-orthopyroxene dacite and minor clinopyroxene-orthopyroxene andesite. The Minmaya rhyolites covering the Kodomari Formation comprise biotite rhyolite, biotite perlite and pumice.

Bulk chemical compositions listed in the appendix show that the Tappi volcanic rocks have wide chemical composition from basalt to rhyolite. Figs. 3 and 4 are K_2O-SiO_2 and FeO*/MgO-SiO_2 diagrams, respectively. The former diagram indicates that the volcanic rocks are mostly plotted in the low- and medium- K andesite fields of Gill's (1981) and some dikes are in the High-K field. Dacitic extrusive rocks of the Horonai Unit are within the calc-alkaline field and the rocks of other units are in both the tholeiitic and calc-alkaline fields (Fig. 4). Basalt and basaltic andesite feeder-dikes of the Tatsuhama Unit, and basaltic dikes and sheets intruding the Horonai and Narugami units are in the tholeiitic field, whereas intermediate and acidic

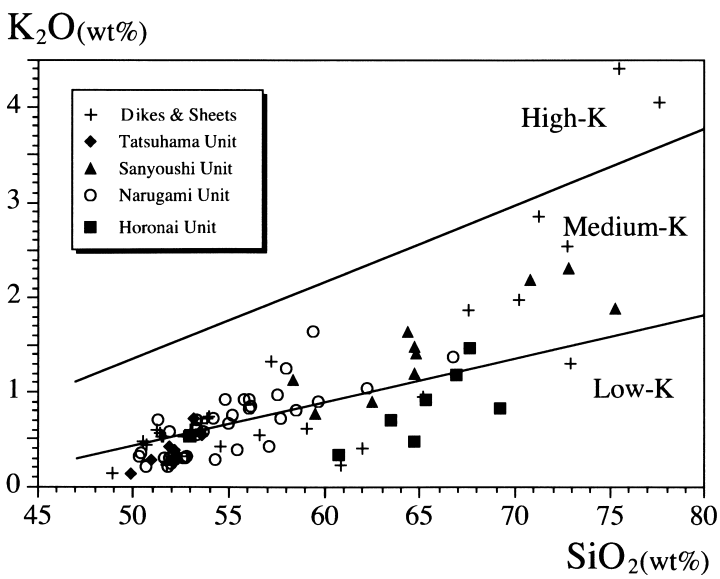

Fig. 3. K_2O vs. SiO_2 variation diagram. Solid lines bound the fields of low-, medium- and high- K orogenic andesites (Gill, 1981) and their extension.

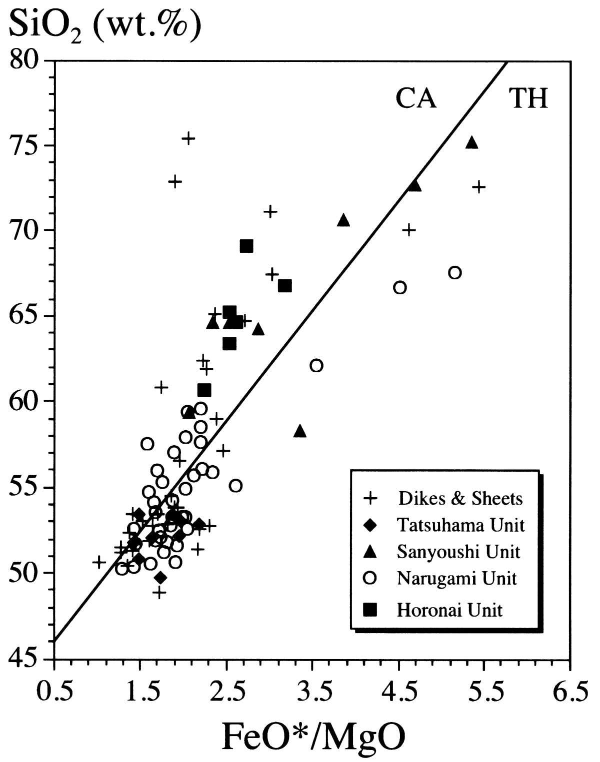

Fig. 4. SiO_2-FeO*/MgO diagram. CA and TH are the fields for calc-alkaline series and tholeiitic series, respectively (Miyashiro, 1974).

dikes intruding the Horonai, Narugami and Sanyoshi units are in the calc-alkaline field.

Basalts and basaltic andesites are enriched in K and Rb and have a negative Nb anomaly on a MORB-normalized incompatible element diagram (Shuto et al., 1995). Their initial $^{87}Sr/^{86}Sr$ ratios (calculated on the basis of K-Ar ages) range from 0.70436 to 0.70479 (Shuto et al., 1993). These petrologic and geochemical characteristics suggest that basaltic rocks of the Tappi volcanics are similar to island arc tholeiites, whereas andesites and more acidic volcanics belong to both the calc-alkaline and island arc tholeiite series.

Sample collection and description

The Tappi volcanic rocks have been altered more or less as mentioned above, requiring the careful sampling and treatment for K-Ar age determination. Then, we tried to collect massive lava samples that are as fresh as possible from the area. As a result, we collected eight lava samples from the Narugami Unit: two basalts (FM05 and NS04) and two andesites (TR04 and KYB01) from the lower part of the unit, three basalts (HLS, UMU03 and MD11) from the middle part and one andesite (TAP15) from the upper part. Two hyaloclastic dacite breccias were also collected from the Horonai (WC14) and Sanyoushi (TAP01) units because there were no fresh lava samples in the units. We also collected six dikes (KS03, NC02, WC31, TP15, KR04 and TP04) and one sheet (TAP14) to compare with the extrusive rocks. Basalt TP04, andesites TAP14 and NC02, dacite TP15 and rhyolite WC31 have intruded into the Horonai Unit, whereas basalts KR04 and KS03, into the Narugami Unit. One rhyolite lava sample was collected from the Minmaya rhyolites. The petrographic features of these rocks are summarized in Table 1.

The basalt and andesite lavas from the Narugami Unit have generally fresh augite and plagioclase as both phenocrysts and groundmass minerals. However, olivine and hyperthene have been altered to saponite, in particular, heavier in the former. The basalt and andesite lavas have various types of groundmass textures: intergranular, hyalopilitic and intersertal. The intersertal groundmasses have volcanic glasses which are partly altered to smectite. It is noted that the andesite TAP15 has the plagioclase phenocysts with lots of fine cracks along which altered minerals occur, and the hyalopilitic groundmass partly altered to smectite.

Hyaloclastic dacite breccias from the Horonai (WC14) and Sanyoushi (TAP01) units contain phenocrysts of fresh augite and plagioclase and of hyperthene with the margin altered to clay minerals, and hyalopilitic groundmass with perlitic cracks and fresh plagioclases. The volcanic glasses in both samples are altered to smectite, in particular, heavily in the TAP01 dacite. Plagioclase in the groundmass is fresh.

The dike and sheet samples have phenocryst assemblages, groundmass textures and alterations similar to the lava samples though two basalts TP04 and KR04 have subophitic groundmass. Rhyolite MN02 from the Minmaya rhyolites comprises phenocrysts of quartz and altered biotite replaced by smectite, with hyalopilitic groundmass composed of plagioclases (fresh) and glasses.

Table 1. Sample list for K-Ar age determination.

Samples	Occurrence	Location	Mineral assemblage	Groundmass texture
Minmaya Rhyolites				
MN02	Lava	41°11' 5" N, 140°25' 8" E	Bt bearing rhyolite	Hyalopilitic textute
Tappi Volcanic Rocks				
Dike&Sheet				
KS03	Dike	41°11' 17" N, 140°23' 16" E	Cpx-opx basalt	Intersertal texture
NC02	Dike	41°13' 16" N, 140°20' 15" E	Opx-Cpx andesite	Hyalopilitic textute
WC31	Dike	41°12' 52" N, 140°20' 9" E	Opx bearing rhyolite	Hyalopilitic textute
TP15	Dike	41°15' 6" N, 140°20' 39" E	Opx-Cpx dacite	Hyalopilitic textute
TAP14	Sheet	41°14' 24" N, 140°20' 40" E	Opx-Cpx andesite	Intersertal texture
KR04	Dike	41°12' 42" N, 140°21' 19" E	Ol bearing Cpx basalt	subophitic texture
TP04	Dike	41°15' 27" N, 140° 20' 43" E	Ol-Cox basalt	subophitic texture
Sanyoushi Unit				
TAP01	Hyaloclastic breccia	41°14' 12" N, 140°23' 27" E	Opx-Cpx dacite	Hyalopilitic textute
Narugami Unit				
MD11	Lava	41°14' 11" N, 140°22' 44" E	Cpx-Opx bearibg Ol basalt	Intersertal texture
UMU03	Lava	41°13' 49" N, 140°22' 35" E	Cpx-Ol basalt	Intersertal texture
HLS	Lava	41°15' 0" N, 140°21' 15" E	Cpx-Ol basalt	Intersertal texture
TR04	Lava	41°13' 36" N, 140°21' 0" E	Opx-Cpx andesite	Intersertal texture
TAP15	Lava	41°14' 40" N, 140°20' 59" E	Cpx-Opx andesite	Hyalopilitic textute
KYB01	Lava	41°12' 4" N, 140°21' 0" E	Cpx andesite	Intersertal texture
NS04	Lava	41°13' 24" N, 140°21' 39" E	Ol bearing Cpx-Opx basalt	Intersertal texture
FM05	Lava	41°14' 1" N; 140°21' 19" E	Opx-Ol bearing Cpx basalt	Integranular texture
Horonai Unit				
WC14	Hyaloclastic breccia	41°13' 17" N, 140°20' 4" E	Opx-Cpx dacite	Hyalopilitic textute

K-Ar age determination

K-Ar age determination of the volcanic rocks has been carried out on the groundmass rich fraction and the plagioclase phenocryst separated from eighteen rock samples of which the localities are given in Fig. 1. The rock samples were crushed and sieved to take 60-80 mesh fractions. Fe-Ti oxides and plagioclase phenocysts were removed from the fraction by a hand magnet and a magnetic separator to concentrate the groundmass rich fraction to be dated. The plagioclase phenocryst for dating was concentrated using the finer grained materials according to the size and texture of phenocrysts. The groundmass rich fraction and the plagioclase phenocrysts were treated with warm 10%-HCl acid to decompose alteration minerals as possible, and then washed repeatedly by distilled water.

Potassium was analyzed using the conventional flame photometry described by Nagao et al. (1984) and Nagao and Itaya (1988) for the groundmass rich fraction and the low K analytical method developed by Itaya et al. (1996) for the plagioclase phenocrysts and some groundmass rich fractions which are extremely low in K. The low K method makes it possible to analyze potassium as low as 0.001 wt. % for the rocks and minerals within about 1% blank contribution to sample potassium. Argon was analyzed by a 15 cm radius sector type mass spectrometer with a single-collector system at Okayama University of Science using an isotope dilution method and an Argon-38 spike (Itaya et al., 1991). Mass discrimination was checked with atmospheric argon several times each day. The specimen was wrapped in Al foil and pre-heated for about 24 hours at 150-200˚C, and followed by argon extraction at 1,500˚C in an ultra-high vacuum line. Reactive gasses were removed using a Ti-Zr scrubber. The decay constants for ^{40}K to ^{40}Ar and ^{40}Ca, and ^{40}K content in potassium used in the age calculation are from Steiger and Jäger (1977) and are 0.581×10^{-10}/y, 4.962×10^{-10}/y and 0.0001167, respectively.

Results and discussion

1. K-Ar ages of whole rock and plagioclase of the Tappi volcanic rocks

As shown in Tables 2 and 3, most K-Ar ages of whole rock are not consistent with those of plagioclase. The differences between whole rock and plagioclase K-Ar ages for each sample are shown in Fig. 5. This figure shows that whole rock K-Ar ages tend to be younger than plagioclase K-Ar ages except for two samples (TAP15, WC14).

It is possible that the discordance between the whole rock and plagioclase K-Ar ages is caused by alteration and hydration. Several researches on radiogenic ^{40}Ar loss and alkali mobility during these processes were already carried out (e.g., Kaneoka, 1972; Mankinen and Dalrymple, 1972; Cerling et al., 1985). Kaneoka (1972) indicated that the increase of H_2O (+) content in rocks was accompanied by radiogenic ^{40}Ar loss during hydration, which resulted in the younger whole rock K-Ar ages than the ages expected from the geological sequence. Mankinen and Dalrymple (1972) pointed out that basalts containing glass were usually unsuitable for K-Ar dating, as critical phases containing K_2O were fine-grained plagioclase and glass based on the observation using electron microprobe. Cerling et al. (1985) also suggested the high degree of alkali mobility during low-temperature alteration of glass for the K-Ar age dating.

It is also suggested from the previous works that the alteration process may not only release radiogenic ^{40}Ar from primary minerals and glasses but also redistribute potassium in altered rocks. In particular, the glass seems to be readily altered to more stable phases, smectite or other clay minerals during alteration and hydration.

Therefore, particular attention should be given in the groundmass texture of the Tappi volcanic rocks. Intergranular and subophitic groundmasses in these rocks are composed of fine-grained minerals such as plagioclase, augite, hyperthene and/or olivine. Basalts TP04 and KR04 with subophitic groundmass show similarity in K-Ar ages within analytical errors between whole rock and plagioclase. Intersertal groundmass in the Tappi volcanic rocks consists of such fine-grained minerals and various amounts of glass. On the other hand, hyalopilitic groundmass in these rocks consists mostly of glass. Most basalts and andesites with intersertal or hyalopilitic groundmass show age differences between whole rock and plagioclase (Fig. 5). Fig. 6 shows that the amounts of loss on ignition (L.O.I.) expressed

Table 2. K-Ar ages of whole rock samples from the Tappi volcanic rocks and the Minmaya rhyolites.

	K (%)	Rad. ^{40}Ar	K-Ar age	Non Rad. Ar (%)
Minmaya Rhyolites				
MN02	4.04±0.08	124.1±1.5	7.9±0.2	17.3
Tappi Volcanic Rocks				
Dike & Sheet				
KS03	0.19±0.01	6.7±0.2	9.0±0.3	43.6
NC02	0.18±0.01	6.3±0.3	9.0±0.6	65.1
WC31	0.87±0.03	31.5±1.2	9.3±0.4	66.4
TP15	1.73±0.04	65.8±1.0	9.8±0.2	30.7
TAP14	0.41±0.02	18.4±0.1	11.5±0.9	78.6
KR04	0.45±0.02	24.7±0.4	14.0±0.7	40.1
TP04	0.46±0.02	25.7±0.5	14.4±0.8	43.0
Sanyoushi Unit				
TAP01	1.31±0.03	28.2±6.2	5.5±1.2	93.3
Narugami Unit				
MD11	0.26±0.01	10.0±1.1	9.9±1.2	87.0
UMU03	0.26±0.01	11.2±1.1	11.1±1.2	85.9
HLS	0.21±0.01	9.3±1.1	11.5±1.5	88.0
TR04	0.89±0.03	44.8±0.6	12.9±0.4	20.8
TAP15	0.52±0.02	26.8±0.5	13.3±0.5	42.6
KYB01	1.23±0.03	64.4±0.9	13.4±0.3	25.1
NS04	0.15±0.01	6.3±1.4	10.9±0.6	47.4
FM05	0.47±0.02	26.9±0.4	14.5±0.8	31.6
Horonai Unit				
WC14	0.56±0.02	32.0±5.6	14.7±2.6	91.3

Table 3. K-Ar ages of plagioclase separates from the Tappi volcanic rocks.

	K (%)	Rad. ^{40}Ar	K-Ar age	Non Rad. Ar (%)
Tappi Volcanic Rocks				
Dike & Sheet				
KS03	0.099±0.005	4.8±0.2	12.5±0.8	63.9
NC02	0.130±0.007	7.6±0.2	15.0±0.9	55.1
WC31	0.713±0.036	34.4±2.2	12.4±1.0	78.8
TP15	0.540±0.027	23.0±0.7	11.0±0.6	57.3
TAP14	0.113±0.006	6.4±0.5	14.4±1.4	82.5
KR04	0.256±0.013	15.2±0.5	15.2±0.9	59.3
TP04	0.235±0.012	13.2±0.4	14.4±0.9	61.8
Sanyoushi Unit				
TAP01	0.200±0.010	7.4±1.1	9.7±1.5	89.9
Narugami Unit				
MD11	0.048±0.002	2.7±0.3	14.6±1.6	85.1
UMU03	0.052±0.003	3.0±0.6	14.6±2.9	92.2
HLS	0.051±0.003	2.9±0.3	14.6±1.7	85.4
TR04	0.079±0.004	4.9±0.3	15.8±1.2	77.4
TAP15	0.096±0.005	4.1±0.4	10.9±1.2	84.0
KYB01	0.205±0.010	13.2±0.3	16.5±0.9	42.9
NS04	0.064±0.006	3.4±0.1	13.4±1.4	65.5
Horonai Unit				
WC14	0.162±0.008	8.2±0.4	12.9±1.0	74.5

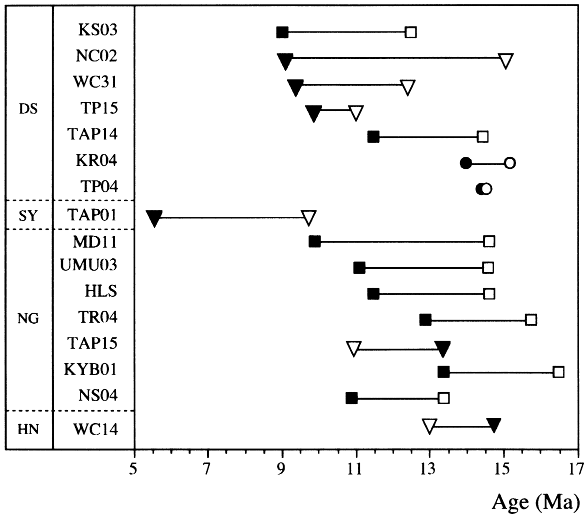

Fig. 5. Differences in K-Ar ages between whole rock and plagioclase separates from the Tappi volcanic rocks. ●○ : samples with subophitic groundmass, ■□ : samples with intersertal groundmass, ▼▽ : samples with hyalopilitic groundmass. Solid and open symbols show whole rock and plagioclase K-Ar ages, respectively. HN: Horonai Unit, NG: Narugami Unit, SY: Sanyoushi Unit, DS: dike and sheet.

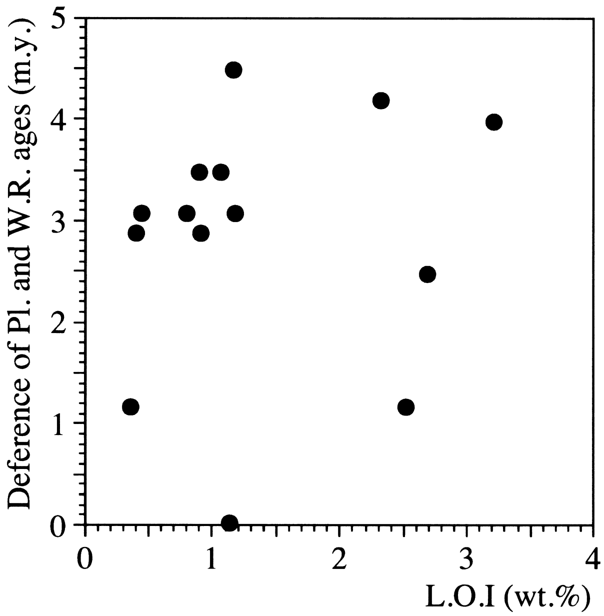

Fig. 6. Relationship between loss on ignition (L.O.I.) and K-Ar age differences between whole rock (W.R.) and plagioclase (Pl.) from the Tappi volcanic rocks.

as H_2O+ content in chemical analyses do not correlate with age differences between whole rock and plagioclase. This phenomenon may be explained by the following features; the low-temperature alteration may have increased L.O.I. in the rocks, as both glass and mafic minerals including olivine and hyperthene in the rocks are easily replaced by clay minerals due to this process. Alteration of mafic minerals, however, will not affect whole rock K-Ar age, because these minerals usually contain negligible amount of K.

Consequently, petrographic observation of the groundmass texture seems to give a good index to select samples for the whole rock K-Ar age determination, although it is impossible to quantitatively evaluate the degree of alteration or hydration by this method. Special attention also needs to determine the K-Ar age for weakly altered volcanic rocks with intersertal or hyalopilitic groundmass, even though these rocks seem to be comparatively fresh.

2. Formation ages of the Tappi volcanic rocks and the Minmaya rhyolites

Comparing the results of the present K-Ar age determination and the previous stratigraphical studies of the Tappi-zaki area (e.g., Ota et al., 1957; Tsushima and Uemura,1959; Japan Railway Construction Corporation, Seikan Branch,1989; Motoyama and Maruyama,1996), the plagioclase K-Ar ages in Table 3 are considered to be close to the formation ages of the Tappi volcanic rocks, although plagioclases in the volcanic rocks were not necessarily formed at the same time as the eruption of these volcanic rocks. Besides, it seems most likely that an incompatible element K is normally concentrated both in the margin of plagioclase phenocryst and in the groundmass plagioclase laths formed at the latest stage of crystallization of constituent minerals of rock, considering the potassium distribution coefficient (= 0.17 to 0.10) between plagioclase and basaltic to rhyolitic melt (Rollinson, 1993). This is another reason why we adopt the plagioclase K-Ar ages as the formation ages of the Tappi volcanic rocks. While the plagioclase K-Ar ages from the Tappi volcanic rocks are within the range from 16.5 to 10 Ma, the ages of the main volcanism in the Tappi-zaki area are considered to be 16.5 to 14 Ma because the Narugami Unit predominates in the volcanic sequence.

The ages of respective Units are interpreted as follows.

(1) Horonai Unit

The Horonai Unit stratigraphically interfingers with the Narugami Unit. Dacite WC14 from the Horonai Unit gave the plagioclase K-Ar age of 12.9±1.0 Ma which is younger than its whole rock K-Ar age of 14.7±2.6 Ma. We interpreted that both the K-Ar ages are nearly identical within analytical errors. Andesite sample TR04 collected from a lava of the Narugami Unit, which overlies the Horonai Unit, yielded the plagioclase K-Ar age of 15.8±1.2 Ma, and another andesite sample NC02 collected from a dike intruding into the latter unit yielded the plagioclase K-Ar age of 15.0±0.9 Ma. Considering these plagioclase K-Ar age data and stratigraphic relationship between the Horonai and Narugami units, the possible formation age of the Horonai Unit ranges from about 16 Ma to 13 Ma.

(2) Narugami Unit

We determined K-Ar ages for eight whole rock samples from this unit and seven plagioclases separated from these samples (Tables 2 and 3). In most samples except basalt sample FM05, the whole rock K-Ar ages tend to be younger compared with K-Ar ages of the plagioclase separates from the same samples (Table 2 and 3, Fig.5). The groundmass of basalt FM05 is intergranular, whereas that of other samples is intersertal or hyalopilitic (Table 1).

Two andesite lava samples, KYB01 and TR04, have similar plagioclase K-Ar ages of around 16 Ma within analytical errors. As an andesite lava from which sample KYB01 was taken overlies the Miocene Fuyube Formation composed of greenish grey tuffaceous sand, its plagioclase K-Ar age (16.5±0.9 Ma) may correspond to the formation age of the base of the Narugami Unit. The plagioclase separates from three basalt samples, UMU03, MD11 and HLS, yielded similar K-Ar ages of 14.6±2.9 Ma, 14.6±1.6 Ma and 14.6±1.7 Ma. The plagioclase of basalt NS04 gave a K-Ar age of 13.4±1.4 Ma which is similar to the above three plagioclase K-Ar ages within analytical errors. Basalt lava sample FM05 contains phenocrysts of fresh augite, hyperthene, plagioclase and altered olivine, and has intergranular groundmass composed mainly of fresh plagioclase with subordinate amounts of augite and Fe-Ti oxides. Thus, the whole rock K-Ar age for sample FM05 may be dominated by plagioclase and pyroxene, having extremely low abundance of K. Consequently, the obtained whole rock K-Ar age of 14.5±0.8 Ma for this sample may be close to its plagioclase K-Ar age (formation age of this basalt lava). The andesite sample TAP15, collected from a lava constituting the uppermost part of the Narugami unit, yielded different whole rock and plagioclase K-Ar ages of 13.3±0.5 Ma and 10.9±1.2 Ma, respectively. The reason why the plagioclase K-Ar age is younger than the whole rock K-Ar age for the andesite is ambiguous. In this paper, we regarded the plagioclase K-Ar age as the formation age. We conclude that volcanic rocks in the Narugami Unit formed during 16.5 to 11 Ma, especially the volcanism was predominant during 16.5 to 14 Ma.

(3) Sanyoushi Unit

A dacite TAP01 showed younger whole rock K-Ar age of 5.5±1.2 Ma which is inconsistent with K-Ar age (9.7±1.5 Ma) of the plagioclase separates from the same sample. Based on the above mentioned characteristics of the groundmass texture of this sample, the younger whole rock age is clearly ascribed to radiogenic ^{40}Ar loss due to alteration of the groundmass. The plagioclase K-Ar age is, therefore, close to the formation age of its host dacite TAP01.

(4) Dikes and sheets

Six dike rocks (TP04, NC02, TP15, WC31, KR04 and KS03) and one sheet rock (TAP14) gave the plagioclase K-Ar ages ranging from 11.0±0.6 Ma to 15.2±0.9Ma (Table 3). The whole rock and plagioclase K-Ar ages of basalt TP04 are almost identical, and both the K-Ar ages of basalt KR04 are also similar each other within analytical errors (Tables 2 and 3). These basaltic rocks show subophitic texture. Other samples (basalt KS03, andesites TAP14 and NC02, dacite TP15 and rhyolite WC31) have intersertal or hyalopilitic groundmass (Table 1), and yielded the whole rock K-Ar ages from 9.0±0.6 to 11.5±0.9 Ma which are younger than K-Ar ages from 11.0±0.6 to 15.0±0.9 Ma for the plagioclase separates from the same samples (Tables 2 and 3). These five plagioclase K-Ar ages seem to represent the formation ages of the dike and sheet rocks.

(5) Minmaya rhyolites

Rhyolite MN02 gave a whole rock K-Ar age of 7.9±0.2Ma. The Minmaya rhyolites overlie the Kodomari Formation composed mainly of mudstone. Motoyama and Maruyama (1996) indicated, using radioralian and diatom biostratigraphy, that the formation age of the uppermost part of the Kodomari Formation ranges from 10.0 Ma to 8.5 Ma. This stratigraphic relationship between the Kodomari Formation and Minmaya rhyolites is consistent with the result of the present K-Ar dating that the Minmaya rhyolites (about 8 Ma) is slightly younger than the uppermost part of the Kodomari Formation. Thus, the whole rock K-Ar age for rhyolite MN02 can be regarded as the formation age of this rhyolite.

Conclusions

1. The K-Ar ages of whole rock and the plagioclases separates were determined for Miocene volcanic rocks from the Tappi-zaki area, Tsugaru Peninsula in the Northeast Japan arc. The whole rock and plagioclase K-Ar ages for basalts with subophitic groundmass are identical within analytical errors, whereas volcanic rocks with intersertal or hyalopilitic groundmass show that the K-Ar ages for whole rocks tend to be younger than those for the plagioclase separates from the same samples. It is interpreted that the obtained younger whole rock K-Ar ages with intersertal or hyalopilitic groundmass may be attributed to the radiogenic ^{40}Ar loss due to alteration and/or hydration of glass in the groundmass. Thus, we adopted the plagioclase K-Ar ages as the formation ages of the host volcanic rocks.
2. Based on the present K-Ar determination, the 1,500 meters thick volcanic rocks from the Tappi-zaki area were produced by the volcanic activity of a relatively long period in the Middle Miocene to Late Miocene, between 16.5 Ma and 10 Ma. Dike and sheet rocks gave K-Ar ages of 15-11 Ma which are coincidental to those of the extrusive members, indicating that both extrusive and intrusive rocks were formed by the same magmatic episode.
3. The obtained whole rock K-Ar age of 7.9±0.2 Ma for the Minmaya rhyolites may represent the formation age of the rhyolites, because the age datum is consistent with the results of stratigraphy of the surrounding area.

References

Cerling, T. E., Brown, F. H. and Bowman, J. R., 1985, Low-temperature alteration of volcanic glass: Hydration, Na, K, ^{18}O and Ar mobility. *Chem. Geol.*, **52**, 281-293.

Gill, J. E., 1981, *Orogenic Andesites and Plate Tectonics.* Springer, Berlin, 390 p.

Itaya, T., Nagao, K., Inoue, K., Okada, T. and Ogata, A., 1991, Argon isotope analysis by a newly developed mass spectrometric system for K-Ar dating. *Mineral. J.*, **15**, 203-221.

Itaya, T., Doi, M. and Ohira, T., 1996, Very low potassium analysis by flame photometry using ultra low blank chemical lines: an application of K-Ar method to ophiolites. *Geochem. J.*, **30**, 31-39.

Japan Railway Construction Corporation, Seikan Branch,1989, Geological map of the Seikan Tunnel, Japan.

Kaneoka, I., 1972, The effect of hydration on the K/Ar ages of volcanic rocks. *Earth. Planet. Sci. Lett.*, **14**, 216-220.

Mankinen, E. A. and Dalrymple, G. B., 1972, Electoron microprobe evaluation of terrestrial basalts for whole rock K-Ar dating. *Earth Planet. Sci. Lett.*, **17**, 89-94.

Miyashiro, A., 1974, Volcanic rock series in island arcs and active continental margins. *Amer.*

J. Sci., **274**, 321-355.

Motoyama, I. and Maruyama, T., 1996, Integrated radiolarian and diatom biostratigraphy of the Neogene strata in the Tsugaru Peninsula, Aomori Prefecture, northern Honshu, Japan. *J. Geol. Soc. Japan*, **102**, 481-499.

Nagao, K. and Itaya, T., 1988, K-Ar determination. *Mem. Geol. Soc. Japan*, no. **39**, 5-21.

Nagao, K., Nishino, H., Itaya, T. and Ogata, K., 1984, An age determination by K-Ar method. *Bull. Hiruzen Res. Inst. Okayama Univ. of Sci.*, no. 9, 19-38.

Ohki, J., Shuto, K., Watanabe, N. and Itaya, T., 1993a, K-Ar ages of the Miocene Ryozen basalts from the northern margin of the Abukuma Highland, Japan. *J. Min. Pet. Econ. Geol.*, **88**, 313-319.

Ohki, J., Watanabe, N., Shuto, K. and Itaya, T., 1993b, Shifting of the volcanic fronts during Early to Late Miocene in the Northeast Japan arc. *The Island Arc*, **2**, 87-93.

Ota, R., Ozawa, A. and Ono, K., 1957, *Geology of the Mimmaya district.* With Geological Sheet Map at 1:50,000, Geol. Surv. Japan, 30 p.

Rollinson, H. R., 1993, *Using Geochemical Data: Evaluation, Presentation, Interpretation*. Longman Singapore Publ. Ltd., 352 p.

Shuto, K., Ohki, J., Kagami, H., Yamamoto, M., Watanabe, N., Yamamoto, K., Anzai, N. and Itaya, T., 1993, The relationships between drastic changes in Sr isotope ratios of magma sources beneath the NE Japan arc and the spreading of the Japan Sea back-arc basin. *Mineral. Petrol.*, **49**, 71-90.

Shuto, K., Nakajima, S., Ohki, J., Uematsu, M., Watanabe, N. and Yamamoto, M., 1995, High field strength element depletions in the lithospheric mantle beneath the Northeast Japan arc. *Mem. Geol. Soc. Japan*, no. 44, 241-262.

Steiger, R. and Jäger, E., 1977, Subcommision on geochronology: convention on the use of decay constants in geo- and cosmo- chronology. *Earth Planet Sci. Lett.*, **36**, 359-362.

Tsushima, K. and Uemura, F., 1959, *Geology of the Kodomari district.* With Geological Sheet Map at 1:50,000, Geol. Surv. Japan, 32 p.

Uto, K., Shibata, K. and Uchiumi, S., 1989, K-Ar ages of Neogene volcanic rocks from Northeast Japan: 1.the Mitaki and Takadate Formations from Sendai district, Miyagi Prefecture. *J. Geol. Soc. Japan*, **95**, 867-872.

Watanabe, N., Takimoto, T., Shuto, K. and Itaya, T., 1993, K-Ar ages of the Miocene volcanic rocks from the Tomari area in the Shimokita Peninsula, Northeast Japan arc. *J. Min. Pet. Econ. Geol.*, **88**, 352-358.

Appendix

Bulk chemical compositions of the Tappi volcanic rocks

Sample	QU01	TR02	WC14	UH01	HR03	TP11B	AN05
Unit	Horonai	Horonai	Horonai	Horonai	Horonai	Horonai	Horonai
SiO_2	67.06	58.80	61.31	61.75	62.39	64.34	67.46
TiO_2	0.61	0.87	0.84	0.78	0.95	0.82	0.85
Al_2O_3	15.13	16.74	15.71	15.84	18.07	15.85	16.37
FeO*	3.64	6.56	5.79	5.08	4.78	5.07	3.30
MnO	0.12	0.17	0.14	0.14	0.16	0.16	0.11
MgO	1.33	2.92	2.28	1.94	1.34	1.99	0.63
CaO	4.66	7.11	6.45	6.46	7.54	5.03	5.41
Na_2O	3.37	3.04	3.08	2.72	3.75	4.06	3.95
K_2O	0.80	0.32	0.68	0.45	1.03	0.90	1.45
P_2O_5	0.13	0.16	0.17	0.20	0.15	0.18	0.14
L.O.I.	2.25	2.74	2.70	4.06	0.44	1.58	0.57
TOTAL	99.10	99.43	99.15	99.42	100.60	99.98	100.24

Sample	WC12	FM04	FM05	FM07	BN11	UMU03	MD11
Unit	Horonai	Narugami	Narugami	Narugami	Narugami	Narugami	Narugami
SiO_2	63.93	52.50	52.75	53.49	54.16	51.90	50.97
TiO_2	0.83	0.94	0.91	0.93	1.01	0.91	1.02
Al_2O_3	14.96	18.29	17.99	18.16	18.29	18.96	19.63
FeO*	4.34	9.51	9.31	8.12	9.02	8.85	8.60
MnO	0.11	0.18	0.17	0.15	0.14	0.16	0.22
MgO	1.36	4.76	4.93	4.89	4.44	4.31	4.42
CaO	5.40	9.29	9.63	9.53	8.26	10.76	10.54
Na_2O	3.22	2.15	2.38	2.43	2.29	2.18	2.63
K_2O	1.11	0.53	0.60	0.71	0.66	0.30	0.28
P_2O_5	0.19	0.11	0.11	0.14	0.14	0.11	0.15
L.O.I.	4.87	0.99	0.71	0.96	1.23	1.07	1.17
TOTAL	100.32	99.25	99.49	99.51	99.64	99.51	99.63

Sample	OM12	KY26	QU05A	QU07	TP23A	EC02B	EC03
Unit	Narugami	Narugami	Narugami	Narugami	Narugami	Narugami	Narugami
SiO_2	56.27	51.93	66.02	54.78	49.37	51.72	51.79
TiO_2	0.91	0.93	0.92	0.94	0.86	1.02	1.01
Al_2O_3	20.19	19.48	16.86	18.11	17.87	18.78	18.71
FeO*	5.40	8.24	3.40	7.44	9.34	8.99	9.13
MnO	0.06	0.15	0.15	0.32	0.21	0.24	0.25
MgO	2.45	4.42	0.76	3.18	7.25	5.15	5.44
CaO	8.68	10.17	5.63	8.90	10.66	10.11	10.15
Na_2O	2.63	2.40	3.55	2.96	1.94	2.56	2.66
K_2O	0.69	0.31	1.36	0.89	0.31	0.27	0.25
P_2O_5	0.13	0.14	0.16	0.14	0.14	0.14	0.15
L.O.I.	1.81	0.94	0.83	1.59	1.25	0.91	1.02
TOTAL	99.22	99.11	99.64	99.25	99.20	99.89	100.56

Sample	EC05	MU11	MU14	KYB01	TR04	KR01	AN04
Unit	Narugami	Narugami	Narugami	Narugami	Narugami	Narugami	Narugami
SiO_2	51.18	57.83	56.06	57.32	57.28	50.14	54.61
TiO_2	0.99	0.95	0.82	1.06	0.81	0.97	0.92
Al_2O_3	18.92	16.35	17.69	17.01	18.29	19.72	17.60
FeO*	9.11	7.49	7.49	8.09	6.29	8.87	8.21
MnO	0.24	0.17	0.18	0.14	0.17	0.19	0.18
MgO	4.99	3.39	3.95	3.98	3.98	5.45	4.65
CaO	10.00	6.98	8.47	6.74	8.02	10.55	9.05
Na_2O	2.55	2.57	2.78	2.95	3.41	2.58	2.68
K_2O	0.28	0.86	0.41	1.23	0.95	0.21	0.38
P_2O_5	0.14	0.17	0.13	0.18	0.14	0.15	0.13
L.O.I.	1.22	2.50	1.48	1.18	0.92	1.37	1.63
TOTAL	99.62	99.26	99.46	99.88	100.26	100.20	100.04

Appendix (continued)

Sample	TB03	TAP15	HLS	FM08	NS04	PT06	MU20
Unit	Narugami	Narugami	Narugami	Narugami	Narugami	Narugami	Narugami
SiO_2	53.07	55.88	52.15	55.80	51.36	55.88	58.28
TiO_2	0.93	0.99	0.96	0.91	0.88	0.96	0.90
Al_2O_3	18.44	20.07	18.73	17.84	19.43	19.81	18.33
FeO*	8.70	6.33	8.83	7.90	8.05	6.63	5.38
MnO	0.17	0.15	0.18	0.20	0.16	0.16	0.18
MgO	5.17	2.83	5.11	4.63	5.51	3.11	2.62
CaO	9.21	8.81	9.97	8.09	10.51	8.90	6.26
Na_2O	2.34	3.36	2.70	3.11	2.75	3.51	4.25
K_2O	0.57	0.84	0.29	0.83	0.20	0.91	1.60
P_2O_5	0.15	0.16	0.13	0.13	0.12	0.15	0.15
L.O.I.	0.64	0.75	0.45	0.63	0.48	0.37	2.07
TOTAL	99.39	100.17	99.50	100.07	99.45	100.39	100.02

Sample	MU13	PT07	KM11	KM16	KS01	HL03	MD10
Unit	Narugami	Narugami	Narugami	Narugami	Narugami	Narugami	Narugami
SiO_2	50.82	55.49	50.07	54.10	57.34	50.22	51.97
TiO_2	0.99	0.99	0.89	0.84	0.77	0.88	0.81
Al_2O_3	18.43	19.64	20.66	18.77	17.92	18.85	17.92
FeO*	9.82	7.76	8.20	6.89	6.35	9.43	8.33
MnO	0.19	0.18	0.20	0.18	0.12	0.22	0.23
MgO	5.52	2.98	4.28	4.26	2.87	6.54	5.81
CaO	10.06	9.49	11.04	9.47	8.56	10.63	10.67
Na_2O	2.25	2.96	2.95	2.97	2.98	2.26	2.40
K_2O	0.69	0.77	0.21	0.91	0.80	0.34	0.30
P_2O_5	0.12	0.13	0.11	0.13	0.11	0.12	0.12
L.O.I.	1.28	0.46	1.29	1.48	1.66	1.16	1.08
TOTAL	100.17	100.85	99.90	100.00	99.48	100.65	99.64

Sample	AN03	FM08	KS04	TAP03	MU03	MD01	EC09
Unit	Narugami	Narugami	Narugami	Narugami	Sanyoushi	Sanyoushi	Sanyoushi
SiO_2	52.97	51.35	52.30	48.31	62.38	59.87	62.20
TiO_2	0.93	0.88	0.81	0.88	0.69	0.84	0.83
Al_2O_3	17.93	18.99	19.99	18.23	17.21	16.35	16.15
FeO*	8.49	8.67	7.61	8.79	4.54	6.18	5.00
MnO	0.17	0.19	0.13	0.14	0.19	0.24	0.14
MgO	4.52	4.75	3.73	7.40	1.58	2.76	1.84
CaO	9.29	10.31	10.11	12.09	5.40	5.29	4.65
Na_2O	2.70	2.97	2.46	1.73	3.15	3.05	3.53
K_2O	0.26	0.56	0.68	0.11	1.57	0.86	1.35
P_2O_5	0.13	0.10	0.11	0.11	0.18	0.25	0.21
L.O.I.	2.42	1.21	1.99	1.44	2.74	3.43	3.21
TOTAL	99.81	99.98	99.92	99.23	99.63	99.12	99.11

Sample	TAP01	FJ06	TAP02	KM04	EC08	MU06	MD02
Unit	Sanyoushi	Sanyoushi	Sanyoushi	Sanyoushi	Sanyoushi	Sanyoushi	Sanyoushi
SiO_2	63.06	58.28	70.73	58.09	63.16	74.08	71.92
TiO_2	0.81	1.13	0.75	0.80	0.82	0.65	0.67
Al_2O_3	16.21	19.46	14.99	18.36	16.16	12.38	14.10
FeO*	4.76	5.92	2.47	5.98	5.08	2.05	2.05
MnO	0.15	0.16	0.11	0.14	0.19	0.13	0.09
MgO	2.03	1.76	0.64	2.87	2.00	0.39	0.44
CaO	4.50	8.38	3.57	7.63	4.53	2.98	2.71
Na_2O	4.18	3.34	4.22	2.81	4.21	3.60	4.21
K_2O	1.44	1.13	2.18	0.76	1.16	1.84	2.28
P_2O_5	0.22	0.18	0.23	0.13	0.22	0.18	0.19
L.O.I.	2.33	0.34	0.38	2.20	2.57	0.83	0.74
TOTAL	99.69	100.08	100.27	99.77	100.10	99.11	99.40

Appendix (continued)

Sample	TAP09	TAP10	EC01	OB01	YO01	TAP08	TAP07
Unit	Tatsudomari	Tatsudomari	Tatsudomari	Tatsudomari	Tatsudomari	Tatsudomari	Tatsudomari
SiO_2	52.58	50.52	52.18	52.58	51.88	49.29	50.30
TiO_2	1.32	1.39	1.32	1.35	1.27	1.25	1.30
Al_2O_3	16.63	17.19	16.60	17.11	16.72	16.10	17.21
FeO*	11.49	11.27	11.29	10.77	11.30	12.59	10.73
MnO	0.20	0.15	0.15	0.12	0.13	0.19	0.17
MgO	5.61	7.24	5.14	5.44	5.79	7.25	7.13
CaO	8.90	7.06	8.75	7.22	8.90	9.44	8.52
Na_2O	2.65	2.80	2.31	3.33	2.66	2.26	2.86
K_2O	0.28	0.49	0.52	0.71	0.31	0.13	0.27
P_2O_5	0.19	0.19	0.17	0.18	0.15	0.14	0.16
L.O.I.	0.77	1.84	0.94	0.76	0.64	0.55	0.99
TOTAL	100.62	100.14	99.37	99.57	99.75	99.19	99.64

Sample	TAP06	TP01	TP02	TAP05	TP13	TP15	WC31
Unit	Tatsudomari	Tatsudomari	Tatsudomari	Tatsudomari	Dike - Sheet	Dike - Sheet	Dike - Sheet
SiO_2	52.57	51.28	52.45	51.39	66.62	69.58	72.34
TiO_2	1.35	1.33	1.33	1.28	0.82	0.80	0.58
Al_2O_3	17.19	17.99	17.44	17.38	16.00	14.92	14.05
FeO*	9.75	9.59	9.64	9.96	3.52	3.21	2.08
MnO	0.12	0.15	0.12	0.12	0.10	0.18	0.11
MgO	5.16	6.64	6.46	6.04	1.16	0.70	1.09
CaO	8.51	8.13	6.91	9.02	4.29	3.99	0.75
Na_2O	2.69	2.98	2.79	2.56	3.99	3.50	6.59
K_2O	0.55	0.42	0.56	0.38	1.83	1.96	1.29
P_2O_5	0.19	0.17	0.17	0.17	0.18	0.20	0.13
L.O.I.	1.09	1.26	1.37	1.20	1.03	0.36	0.80
TOTAL	99.17	99.94	99.24	99.50	99.54	99.40	99.81

Sample	HR12	MU21	TP04	KS03	TP18	TAP14	TB01
Unit	Dike - Sheet	Dike - Sheet	Dike - Sheet	Dike - Sheet	Dike - Sheet	Dike - Sheet	Dike - Sheet
SiO_2	52.43	65.12	51.89	51.72	54.27	58.74	70.57
TiO_2	0.84	0.77	1.31	0.79	0.94	1.03	0.53
Al_2O_3	18.32	17.15	16.32	19.67	18.15	16.98	14.54
FeO*	8.71	3.75	11.69	8.32	8.79	7.66	2.48
MnO	0.14	0.08	0.16	0.16	0.16	0.17	0.10
MgO	5.67	1.58	5.06	5.10	4.71	3.18	0.82
CaO	9.58	7.07	8.74	10.70	8.93	7.44	3.02
Na_2O	2.18	3.10	2.26	2.51	2.77	3.35	3.95
K_2O	0.58	0.94	0.51	0.24	0.42	0.61	2.82
P_2O_5	0.12	0.17	0.17	0.12	0.12	0.16	0.13
L.O.I.	0.77	0.71	1.14	0.90	0.62	0.41	1.12
TOTAL	99.34	100.44	99.25	100.23	99.88	99.73	100.08

Sample	TP16	HR10	TP12	NC02	TP04B	TP14	HR08
Unit	Dike - Sheet	Dike - Sheet	Dike - Sheet	Dike - Sheet	Dike - Sheet	Dike - Sheet	Dike - Sheet
SiO_2	53.50	53.34	53.57	58.66	52.17	50.77	52.10
TiO_2	1.16	0.85	1.16	0.89	1.28	1.27	0.89
Al_2O_3	16.66	18.03	16.58	16.47	17.04	16.66	19.31
FeO*	10.49	8.48	10.58	5.97	11.14	11.84	8.18
MnO	0.18	0.23	0.20	0.17	0.15	0.13	0.20
MgO	5.39	5.96	5.50	3.42	5.05	5.43	4.48
CaO	8.11	9.42	8.20	6.88	8.66	9.58	9.51
Na_2O	2.60	2.55	2.61	3.35	2.75	2.11	2.83
K_2O	0.74	0.60	0.71	0.23	0.52	0.52	0.58
P_2O_5	0.15	0.11	0.14	0.18	0.17	0.14	0.12
L.O.I.	0.80	1.19	0.64	3.21	0.48	0.85	1.75
TOTAL	99.78	100.76	99.89	99.43	99.41	99.30	99.95

Appendix (continued)

Sample	BN08	TP22	QU03	HR04	KM02	NC03	WC13
Unit	Dike - Sheet	Dike - Sheet	Dike - Sheet	Dike - Sheet	Dike - Sheet	Dike - Sheet	Dike - Sheet
SiO_2	52.73	47.84	49.08	50.85	72.81	48.61	52.10
TiO_2	0.91	1.24	0.88	0.83	0.56	1.06	0.85
Al_2O_3	18.65	16.07	16.35	17.18	14.61	16.07	18.10
FeO*	8.19	12.56	9.79	9.21	2.07	9.40	8.97
MnO	0.11	0.20	0.14	0.21	0.07	0.17	0.23
MgO	4.53	7.22	7.17	6.27	0.38	9.17	6.50
CaO	7.04	9.90	11.14	10.92	2.53	8.52	9.50
Na_2O	3.19	2.23	1.81	2.20	4.35	2.15	2.55
K_2O	2.05	0.13	0.46	0.25	2.52	0.42	0.31
P_2O_5	0.10	0.16	0.14	0.11	0.12	0.17	0.11
L.O.I.	2.47	2.23	2.96	1.94	0.56	4.61	0.39
TOTAL	99.97	99.78	99.92	99.97	100.58	100.35	99.61

Sample	WC23	BN09	FJ08	SB02	WC25	TP16	TP05
Unit	Dike - Sheet	Dike - Sheet	Dike - Sheet	Dike - Sheet	Dike - Sheet	Dike - Sheet	Dike - Sheet
SiO_2	55.88	50.56	51.55	56.06	52.89	52.50	77.40
TiO_2	1.35	0.91	0.88	0.89	1.04	0.87	0.28
Al_2O_3	15.76	16.42	18.51	17.42	17.99	17.60	12.37
FeO*	9.25	9.34	8.93	8.30	9.24	9.26	0.97
MnO	0.18	0.15	0.23	0.18	0.22	0.20	0.04
MgO	3.74	7.22	6.10	4.21	5.41	5.62	0.04
CaO	6.70	11.00	10.54	8.38	8.12	10.27	1.29
Na_2O	3.15	2.16	2.28	2.69	2.99	2.52	3.16
K_2O	1.28	0.58	0.21	0.55	0.66	0.31	4.03
P_2O_5	0.21	0.16	0.12	0.13	0.16	0.10	0.05
L.O.I.	1.56	2.13	0.80	1.15	1.50	0.62	0.83
TOTAL	99.06	100.63	100.15	99.96	100.22	99.87	100.46

Sample	KR04	KG14	KR05	TP19	MD04	FJ04	TAP12
Unit	Dike - Sheet	Dike - Sheet	Dike - Sheet	Dike - Sheet	Dike - Sheet	Dike - Sheet	Dike - Sheet
SiO_2	49.95	59.84	50.96	75.64	52.45	48.58	48.50
TiO_2	0.90	0.87	0.93	0.27	1.20	0.80	0.95
Al_2O_3	16.41	15.70	15.97	12.99	17.18	16.61	17.38
FeO*	9.41	6.42	9.19	1.34	7.09	9.57	11.25
MnO	0.14	0.19	0.18	0.04	0.18	0.14	0.20
MgO	6.65	2.80	7.08	0.65	7.34	7.43	7.00
CaO	10.85	6.82	11.69	1.05	8.09	11.81	10.33
Na_2O	2.06	3.12	2.02	3.60	2.40	1.89	2.08
K_2O	0.55	0.40	0.52	4.41	0.82	0.50	0.07
P_2O_5	0.14	0.16	0.15	0.05	0.22	0.13	0.12
L.O.I.	2.52	3.70	2.00	0.56	2.25	1.70	1.24
TOTAL	99.58	100.02	100.69	100.60	99.22	99.16	99.12

Sample	MN02
Unit	Minmaya Rhyolites
SiO_2	76.36
TiO_2	0.15
Al_2O_3	11.69
FeO*	0.89
MnO	0.06
MgO	1.72
CaO	0.1
Na_2O	1.15
K_2O	5.26
P_2O_5	0.02
L.O.I.	2.38
TOTAL	99.78